LA-UR -81-2468

CONF-810439--36

MASTER

Los Alamos National Laboratory is operated by the University of California for the United States Department of Energy under contract W-7405-ENG-36

TITLE OPTICAL ANALYSIS AND ALIGNMENT APPLICATIONS USING THE INFRARED SMARTT INTERFEROMETER

AUTHOR(S) V. K. Viswanathan
P. D. Bolen
I. Liberman, Westinghouse R&D Center, Pittsburgh, PA
B. D. Seery, TRW Inc., Applied Technology Division, Redondo Beach, CA

SUBMITTED TO Los Alamos Conference on Optics '81
Los Alamos, New Mexico
April 1981

Los Alamos
Los Alamos National Laboratory
Los Alamos, New Mexico 87545

A402

Optical analysis and alignment applications using the infrared Smartt interferometer*

V.K. Viswanathan, P. D. Bolen, I. Liberman,** and R. D. Seery***

Los Alamos National Laboratory, University of California
Mail Stop [illegible], P.O. Box 1663, Los Alamos, NM 87545

Abstract

The possibility of using the infrared Smartt interferometer for optical analysis and alignment of infrared laser systems has been discussed previously.[1,2] In this paper, optical analysis of the Gigawatt Test Facility at Los Alamos, as well as a deformable mirror manufactured by Rocketdyne, are discussed as examples of the technique. The possibility of optically characterizing, as well as aligning, pulsed high energy laser systems like Helios and Antares[3] is discussed in some detail.

Introduction

The Smartt interferometer[4] is a common path interferometer which generates its own reference wave, [illegible] by the lens under test. The Smartt plate, [illegible] [illegible] [illegible] [illegible] [illegible] and the reference beam is [illegible] [illegible] [illegible] [illegible] [illegible] 30% [illegible] high contrast fringes [illegible].

The [illegible] interferometer [illegible] [illegible] fringes of constant [illegible] to the [illegible] fringes.

[illegible]

There are two basic types of Smartt interferometer applications which we are pursuing: alignment and optical analysis/evaluation. The typical fringe pattern for alignment [illegible] Fig. 1. [illegible] fringes were taken at the vicinity of the focal plane of [illegible] with a [illegible] μm hole in the Smartt plate. For beams with very little aberration, the Smartt interferometer produces circular dark and white fringes in and out of focus, and straight line fringes when tilt is introduced in the two directions orthogonal to the focus direction. Hence, the problem of locating the proper focus is equivalent to determining the location of a point in space and thus the error in locating this along the focus axis can be considered as a focus error and the error in the other two orthogonal directions is a pointing error. In practice, trying to locate the null fringe is a very insensitive technique to locate focus. If a tilt is introduced, the fringe patterns shown in Fig. 1 are produced. The left column shows the effect of going through focus and the other two correspond to the direction of tilt. The middle row is in the nominal focal plane and the other rows are fringes in increments of [illegible] μm. (Airy disc size is roughly 60 μm.) The curvature changes sign in going through focus and the slant of the fringes changes directions for the pointing cases. Thus, one can locate the focal plane, and actually locate focus by removing the tilt. In practice, this just involves moving the Smartt plate to a different location and bringing it back to the original location, which can be done with accuracy. Figure 2 shows the typical fringe pattern obtained when the Smartt fringes are used for image evaluation purposes. These fringes are digitized and analyzed using the code FRINGE. Apart from the deliberate defocus introduced to get more fringes, the analysis for this particular case showed that the root-mean-square error for the wavefront was 0.11λ at 10.6 μm. This wavefront would produce a Strehl ratio of 0.5 and the major third-order aberrations present are: λ/2 of astigmatism, λ/7 of spherical aberration, and λ/3 of coma. This type of image analysis using Smartt interferograms is illustrated with two examples, one involving the study and

---

*Work performed under the auspices of the U.S. Department of Energy
**Westinghouse R. D. Center, Pittsburgh, Pennsylvania
***TRW Inc., Applied Technology Division, Redondo Beach, California

analysis of the Gigawatt Test Facility (GWTF) in Los Alamos, and the other involving the optical analysis of a deformable mirror manufactured by Rocketdyne.

Optical quality and stability of the reinjection oscillator (RIO) and Lumonics 600 amplifier in the Gigawatt Test Facility (GWTF) at Los Alamos

Figures 3 and 4 show the schematic and the various optical elements in the RIO Lumonics/GWTF system. Typically, a 70-ns CO_2 laser pulse from the oscillator goes through a three-stage electro-optic switch and a 0.2-1 ns pulse (adjustable) emerges. It then makes four passes through the amplifier and emerges with a 400 mJ energy. The beam then goes through a spatial filter, isolator, and a beam expander section (the details are shown in Fig. 4) before going through the Lumonics 600 amplifier. The beam size at the output end of the triple electro-optic switch is 1 cm and the beam size at the output of the Lumonics 600 is 6 cm, and the energy is 3-6 J.

A surrogate laser (CO_2 cw laser) was used along with a focusing lens to produce Smartt interferograms of the various subsystems in the RIO/Lumonics system. The effects of the laser and the focusing lens were subtracted in the computer analysis to compute the contributions of each subsegment. Table 1 shows the results obtained with the RIO, the Lumonics, and the test lens. The third-order spherical aberration and coma contribution for the individual systems (RIO, Lumonics, and Testlens) added up is almost equal to the whole system (after Lumonics, including the RIO, Lumonics, and Testlens). Though the coma and astigmatism need not add up properly (because their angles can be different), this shows that this method appears to work very well indeed. Table 2 shows the typical results from studying the stability of the various sections of the GWTF system. Among the major conclusions reached were: (1) The various parts of the RIO/Lumonics system appear to have reasonable optical stability. (2) The Lumonics appears to have the best and the RIO the worst optical quality. 3) Significant compensation or defects in optical quality takes place in the RIO/Lumonics System.

Table 1. Typical results of analysis of Smartt interferograms

Beam after [illegible]	rms (in λ)	p-v (in λ)	Strehl	70-80% Diameter (mm)	Test Lens Aberrations (in λ units)	
[illegible]	0.09	0.1	0.01	120	SPH	-2.7
[illegible]				109	COMA	+0.7
[illegible]					AST	+0.2
Lumonics	0.11	0.7	0.5	46	SPH	+1.8
				98	COMA	+0.4
					AST	+0.2
Test Lens	0.11	0.6	0.5	51	SPH	+1.5
				82	COMA	+0.1
					AST	0.0
After Lumonics (Whole System including test lens)	0.11	0.8	0.6	34	SPH	-1.0
				67	COMA	+0.7
					AST	+0.2
					Adding:	
					SPH:	-1.2
					COMA:	+0.7
					AST:	+0.4
					(cannot add COMA and AST properly)	

Optical performance evaluation of the Rocketdyne deformable mirror[9]

The deformable mirror built by Rocketdyne was intended to cancel the laser wavefront phase errors caused by the quasi-static aberrations present in large laser systems like the CO_2 laser fusion systems. The mirror consists of a thin mirror face plate supported by 19 differential ball screws which act to deform the faceplate relative to a thick body support structure. The unique differential ball screws, with an effective pitch of 10 μm, act as both position and force actuators. Each screw is driven by a stepper motor giving a surface positioning resolution of 0.075 μm. The ball screw assemblies are preloaded by flexure-type springs so that a high positive tensional load is maintained on the screws over the full range of deflection, ±20 μm. In series with each ball screw is a piezoceramic (PZT) element which provides a ±0.5 μm peak amplitude high-frequency surface dither for the wavefront error correction process. Reference 8 provides a detailed description of the mirror. Ideally, by using a wavefront error sensing system and the 19 actuators, the mirror produces the conjugate wavefront to that produced by the laser system, and thus the resultant wavefront is aberration free.

A402

Table 2. Typical results from studying stability of GWTF system

Description	RMS (in λ)	P-V	Strehl	70-80% Diameter (μm)	3rd Order Aberrations (in λ units)	
810 (without four-pass)						
(A) 9:30 a.m.	0.32	1.4	0.01	240	SPH	-4.3
				308	COMA	+0.3
					AST	+0.7
(B) 11:30 a.m.	0.37	1.5	0.02	240	SPH	-5.2
				295	COMA	+0.9
					AST	+0.7
Lumonics Amplifier						
(A) 1 p.m.	0.14	0.7	0.45	42	SPH	+1.1
				90	COMA	+0.5
					AST	+0.2
(B) 1:30 p.m.	0.14	0.7	0.52	46	SPH	+1.6
				88	COMA	+0.4
					AST	+0.2
After Lumonics (whole system)						
(A) 3 p.m.	0.13	0.8	0.62	34	SPH	-1.0
				67	COMA	+0.7
					AST	+0.2
(B) 3:30 p.m.	0.13	0.8	0.62	34	SPH	-0.7
				67	COMA	+0.2
					AST	+0.5
(C) 5 p.m.	0.10	0.6	0.76	37	SPH	-0.6
				61	COMA	+0.5
					AST	+0.1

Figure 5 shows the experimental setup to test the stability of the mirror and its ability to produce the conjugate wavefront for the types of aberrated wavefronts expected in the laser fusion systems. The Rochdyne deformable mirror was designed to replace the spherical mirror in the triple-pass amplifier in the Helios laser system and hence the experimental setup duplicates the target area of the Helios laser. A 24-cm-diam beam was used in these experiments, and the collimating mirror (25") in Fig. 5 was replaced by the deformable mirror. The expanded beam from a sylvania HeNe laser is cleaned by a spatial filter and expanded to fill the aperture of the deformable mirror. The collimated beam from the deformable mirror is brought to focus by a combination of turning-flat/off axis focusing parabola. The Smartt plate is at the focus, and is capable of three orthogonal displacements in the x, y, and z directions, as it is mounted on an x-y-z stage. The overhead TV vidicon lens images the exit pupil plane (which contains the aberrations of the system) onto the vidicon, yielding a video signal that is displayed on a video monitor. The resulting interference fringes on the monitor appear similar to those in Fig. 2 and represent the optical path difference errors of the system under test. As described in the introduction, these fringes are digitized and analyzed to calculate the optical parameters of interest. Tables 3 and 4 show typical results obtained from the analysis of the Smartt interferograms obtained during the testing of the deformable mirror. The two major characteristics that were studied were the stability of the mirror and the ability of the mirror to correct phase aberrations. In all these cases, the optical parameters in the tables were computed from experimentally produced interferograms. These tests showed that the deformable mirror was optically stable over long periods of time and over temperature variations of 15° F and it was capable of correcting phase aberrations of the type expected in CO_2 laser fusion systems.

Table 3. Stability of the Rochdyne mirror

Description	Diam in Microns for Strehl Ratio	Diam in Microns for 80% Encircled Energy	Diam in Microns for 84% Encircled Energy
(A) 9:30 a.m.	0.54	57	70
(B) 2:00 p.m.	0.52	59	81

Table 4. Ability to correct aberrations

Description	Diam in Microns for Strehl Ratio	Diam in Microns for 80% Encircled Energy	Diam in Microns for 84% Encircled Energy
(A) Initial State	0.61	59	79
(B) Aberrated Wavefront Introduced	0.09	141	164
(C) Corrected State Using Deformable Mirror	0.61	59	88

A402

Possible alignment and optical characterization of pulsed high energy lasers like Helios and Antares

The proposed method for alignment and optical characterization of Antares involves the utilization of Smartt interferometry at the focal plane. Another paper at this meeting[9] describes the use of the Antares Alignment Gimbal Positioner for this purpose. The optical characterization at full power of a high energy pulsed CO_2 Laser (similar to the CO_2 Laser Fusion Systems) is yet to be done. The problem is complicated by the short pulse length (~1 ns) and high energies in the beam (1500 J in 34 cm diam). For infrared applications, the interference pattern impinges upon a pyroelectric vidicon which requires about 50 uJ to be conveniently detected. Typically, 10% transmission results in good contrast fringes and thus the input to the interferometer should be about 0.5 mJ. For the Helios system[10] with an F number of 2.4 and Strehl ratio of 0.6, this implies a peak energy density of 35 J/cm^2. No known material can avoid optical damage at 35 J/cm^2 with nanosecond pulses. As the silicon plate (which the Smartt plate is made of) can withstand roughly only 1 J/cm^2 for 1-ns pulses, the focal spot must be magnified at least a factor of 6 to an F/15 beam. This magnification can readily be achieved with germanium lenses without introducing significant aberrations (and the effects of the germanium lenses subtracted out) so that alignment and beam-quality measurements can be made with an attenuated front-end pulse. It would be very useful to know whether the alignment and energy distribution for the full-power shot is similar to the unamplified front-end beam used in these studies. Through the use of a hole grating, the full-power beam can be altered to an acceptable energy level on the Smartt plate.[11] This scheme has been discussed in some detail previously.[1] A virtue of the Smartt interferometer approach is that it could supply the desired information in a single shot, whereas the other techniques such as the "energy in the bucket" measurements require many shots, which at high power levels are time consuming, stress the amplifiers, and require exceedingly good shot-to-shot reproducibility.

Conclusions

The Smartt interferometer can be used for both the optical alignment and optical assembly, as well as the image evaluation of laser systems. Apart from the fact that it is easy to fabricate and simple to use, it has the additional advantage that optical assembly, optical alignment, and image optimization all can be accomplished simultaneously. In CO_2 laser fusion systems the final focusing element is a decentered paraboloid. Its alignment strongly influences the focal spot beam quality. Therefore, the tasks of alignment and focal spot energy distribution are considerably interrelated. With the use of the Smartt interferometer, alignment and energy distribution can be determined and optimized. The process described here to use the Smartt plate with the proper hole size and attenuation appears to work well with relative ease. The Smartt interferometer itself, because of its simplicity and versatility, emerges as a strong candidate for use in assembly, alignment, and evaluation of high energy laser systems. It also opens up the possibility of detailed optical design and engineering of these systems. The relatively high damage threshold of the silicon bulk absorption Smartt interferometer allows the technique to be practical with CO_2 lasers having pulse durations of nanoseconds.

Acknowledgement

We would like to thank Ms. Lauren Carlson for the interferogram reductions she did for the various infrared Smartt interferograms used in this article.

References

1. V. K. Viswanathan, I. Liberman, G. Lawrence, and R. D. Seery, Applied Optics, Vol. 19, No. 11, 1870 (1980).
2. V. K. Viswanathan and P. D. Rolen, Proc. of the SPIE, Vol. 179, p. 107 (1979).
3. Helios is an 8-beam, 10-kJ, CO_2 laser currently being used at Los Alamos for laser fusion experiments.
4. Antares is a 24-beam, 40-kJ, CO_2 laser currently under construction at Los Alamos.
5. R. H. Smartt and J. Strong, Journal of Scientific Applications 62, 737 (1972). Also R. H. Smartt and W. H. Steel, Journal of Applied Physics Supplement 14, 351 (1975).
6. C. Kolliopoulos, O. Kwon, P. Shagam, and J. C. Wyant, Optics Letters, Vol. 3, p. 118 (1978).
7. FRINGE is an interferogram reduction program developed by J. Loomis while at the University of Arizona Optical Sciences Center.
8. This mirror has been described in detail in the article by W. D .Henderson and S. V. Gunn, Proceedings of the SPIE, Vol. 179, p. 51 (1979).
9. Paper A203 by R. D. Day, V. K. Viswanathan, A. C. Saxman, R. E. Lujan and G. L. Woodfin. LASL Conference on Optics 1981.

A402

10. I. Liberman, 1980 Optical Meeting on Inertial Confinement Fusion, paper TuB 10, San Diego, California, February 1980.
11. J. V. Parker, I. Liberman, and V. K. Viswanathan, paper TuC 3, Conference on Inertial Confinement Fusion, February 1978, San Diego, California.

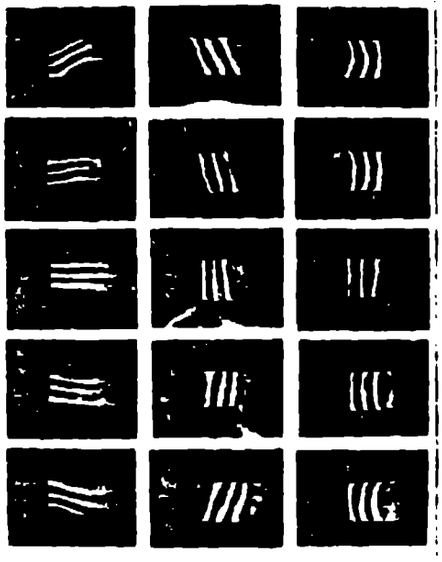

Fig. 1. Typical fringe patterns for alignment.

Fig. 2. Typical fringe pattern for image evaluation.

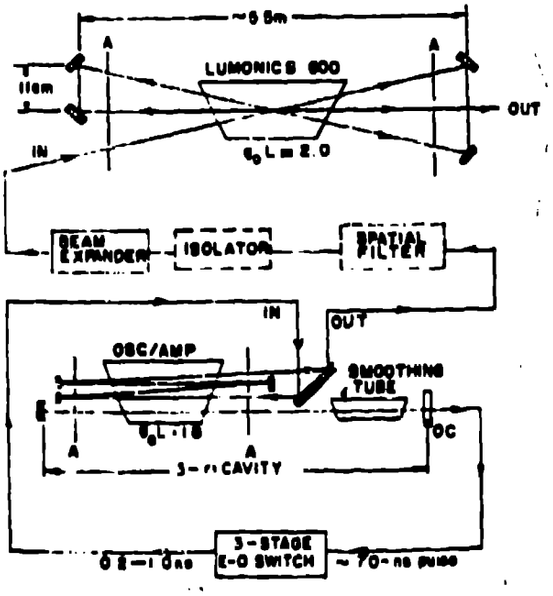

Fig. 3. Schematic of RIO Lumonics/GWTF system.

A402

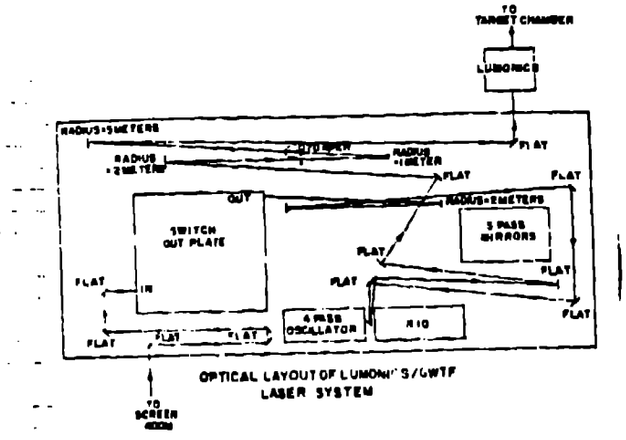

OPTICAL LAYOUT OF LUMONICS/GWTF LASER SYSTEM

Fig. 4. Optical layout of Lumonics/GWTF laser system.

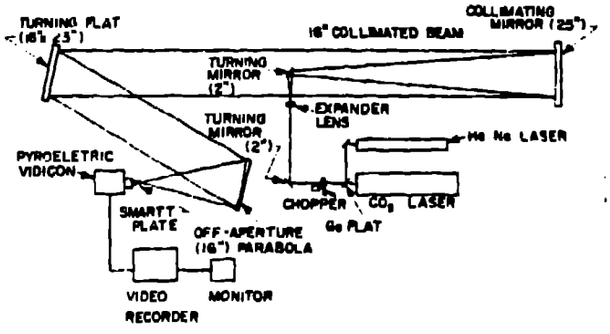

Fig. 5. Experimental setup for testing deformable mirror.